Fetal Growth Restriction Results in Remodeled and Less Efficient Hearts in Children

Fàtima Crispi, Bart Bijnens, Francesc Figueras, Joaquim Bartrons, Elisenda Eixarch, Ferdinand Le Noble, Asif Ahmed and Eduard Gratacós

Circulation. 2010;121:2427-2436; originally published online May 24, 2010;
doi: 10.1161/CIRCULATIONAHA.110.937995
Circulation is published by the American Heart Association, 7272 Greenville Avenue, Dallas, TX 75231

Print ISSN: 0009-7322. Online ISSN: 1524-4539

Fetal Growth Restriction Results in Remodeled and Less Efficient Hearts in Children

Fàtima Crispi, MD; Bart Bijnens, PhD; Francesc Figueras, MD; Joaquim Bartrons, MD; Elisenda Eixarch, MD; Ferdinand Le Noble, PhD; Asif Ahmed, PhD; Eduard Gratacós, MD

Background—Fetal growth restriction (FGR) affects 5% to 10% of newborns and is associated with increased cardiovascular mortality in adulthood. The most commonly accepted hypothesis is that fetal metabolic programming leads secondarily to diseases associated with cardiovascular disease, such as obesity, diabetes mellitus, and hypertension. Our main objective was to evaluate the alternative hypothesis that FGR induces primary cardiac changes that persist into childhood.

Methods and Results—Within a cohort of fetuses with growth restriction identified in fetal life and followed up into childhood, we randomly selected 80 subjects with FGR and compared them with 120 normally grown fetuses, matched for gender, birth date, and gestational age at birth. Cardiovascular assessment was performed in childhood (mean age of 5 years). Compared with control subjects, children with FGR had a different cardiac shape, with increased transversal diameters and more globular cardiac ventricles. Although left ejection fraction was similar among the study groups, stroke volume was reduced significantly, which was compensated for by an increased heart rate to maintain output in severe FGR. This was associated with subclinical longitudinal systolic dysfunction (decreased myocardial peak velocities) and diastolic changes (increased E/E′ ratio and E deceleration time). Children with FGR also had higher blood pressure and increased intima-media thickness. For all parameters evaluated, there was a linear increase with the severity of growth restriction.

Conclusions—These findings suggest that FGR induces primary cardiac and vascular changes that could explain the increased predisposition to cardiovascular disease in adult life. If these results are confirmed, the impact of strategies with beneficial effects on cardiac remodeling should be explored in children with FGR. **(*Circulation*. 2010;121:2427-2436.)**

Key Words: remodeling ■ pregnancy ■ pediatrics ■ cardiomyopathy ■ hypoxia

Cardiovascular disease is the main cause of death in adults. Most factors that lead to chronic cardiovascular disease are already present in childhood.[1,2] Epidemiological evidence has long suggested a link between low birth weight and increased cardiovascular mortality in adulthood.[3] This association is essentially mediated through fetal growth restriction (FGR),[4] a condition defined as a birth weight below the 10th percentile for gestational age that affects 5% to 10% of all newborns.[5] The mechanistic pathways underlying the relationship between FGR and cardiovascular risk are poorly understood.[6] A number of studies support that it might be explained in part by fetal metabolic programming leading to diseases associated with cardiovascular disease, such as obesity, diabetes mellitus, and hypertension[6]; however, it remains unclear whether FGR induces primary changes in the heart that might predispose to cardiovascular dysfunction later in life.

Clinical Perspective on p 2436

It has long been known that intrauterine growth retardation is associated with dilated cardiomyopathy–like changes in utero.[7] Recent studies have demonstrated that fetuses[8,9] and newborns[10] with severe forms of growth restriction have significant changes in fetal cardiac function parameters and natriuretic peptides. In addition, newborns with FGR have an increase in aortic intima-media thickness,[11] which supports

Received September 22, 2009; accepted April 6, 2010.

From the Department of Maternal-Fetal Medicine (Institut Clínic de Ginecologia, Obstetrícia i Neonatologia), Hospital Clinic-IDIBAPS, University of Barcelona, and Centro de Investigación Biomédica en Red en Enfermedades Raras (F.C., F.F., E.E., E.G.), Barcelona, Spain; ICREA-Universitat Pompeu Fabra (CISTIB) and Centro de Investigación Biomédica en Red en Bioingeniería, Biomateriales y Nanomedicina (B.B.), Barcelona, Spain; Department of Pediatric Cardiovascular Surgery, University Hospital Sant Joan de Déu (J.B.), Esplugues de Llobregat, Barcelona, Spain; Laboratory for Angiogenesis and Cardiovascular Pathology, Max Delbrück Center for Molecular Medicine (F.L.N.), Berlin, Germany; Department of Reproductive and Vascular Biology (A.A.), Centre for Cardiovascular Sciences, Institute for Biomedical Research, University of Birmingham, Birmingham, United Kingdom; and Gustav Born Centre for Vascular Biology and Centre for Cardiovascular Sciences (A.A.), Queen's Medical Research Institute, College of Medicine and Veterinary Medicine, University of Edinburgh, Edinburgh, United Kingdom.

The online-only Data Supplement is available with this article at http://circ.ahajournals.org/cgi/content/full/CIRCULATIONAHA.110.937995/DC1.

Correspondence to Eduard Gratacos, Department of Maternal-Fetal Medicine (ICGON), Hospital Clinic, Sabino de Arana 1, 08028, Barcelona, Spain. E-mail egratacos@clinic.ub.es

Circulation **is available at http://circ.ahajournals.org** **DOI: 10.1161/CIRCULATIONAHA.110.937995**

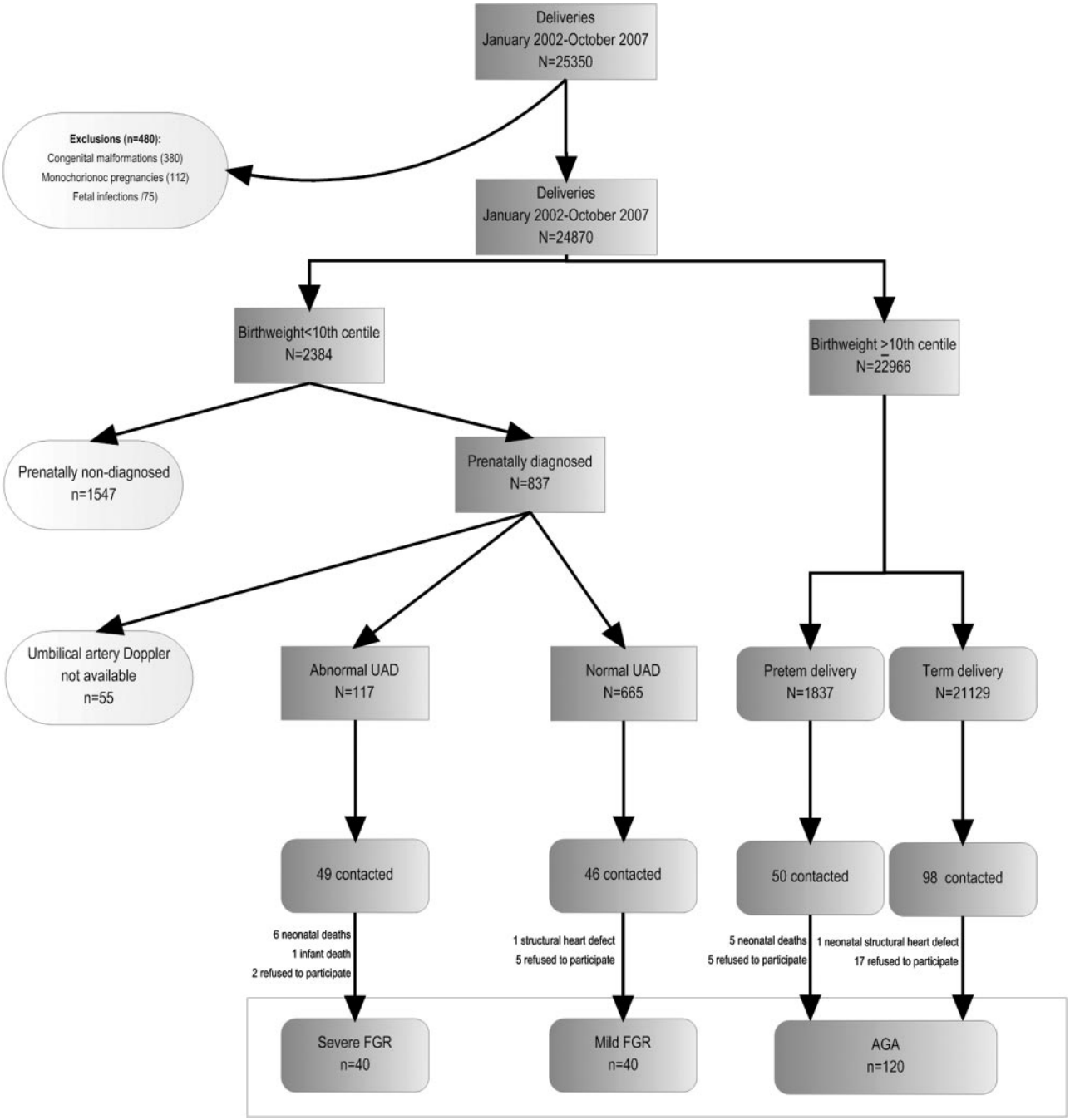

Figure 1. Flow diagram of children in the study groups. AGA indicates control subjects; UAD, umbilical artery Doppler.

the existence of vascular remodeling. Experimental studies suggest that subclinical cardiovascular abnormalities in fetuses exposed to growth restriction persist into adulthood,[12] but it is unknown whether this effect occurs in humans.

In the present study, we evaluated the hypothesis that adaptation to growth restriction induces persistent cardiovascular changes in children. From a prospective perinatal registry, we selected a cohort of FGR children classified into categories as having mild or severe growth restriction, as well as a cohort of normally grown children matched for gestational age at delivery. We evaluated the association between FGR and echocardiographic structural and functional measurements in childhood.

Methods

Study Populations

The study design was a prospective cohort study that included 80 case subjects with FGR and 120 control subjects with birth weight appropriate for gestational age identified in fetal life and followed up into childhood. The source population comprised all pregnancies cared for from January 2002 to October 2007 at a tertiary referral university hospital in Barcelona, Spain, which covers an inner city area of approximately 0.6 million inhabitants, who were registered in a database prospectively constructed at the time of delivery (n=25 350). Case subjects were considered noneligible in the presence of any of the following: Congenital malformations or chromosomal defects, evidence of fetal infection, or multiple monochorionic pregnancy. Eligible case subjects were infants with a birth

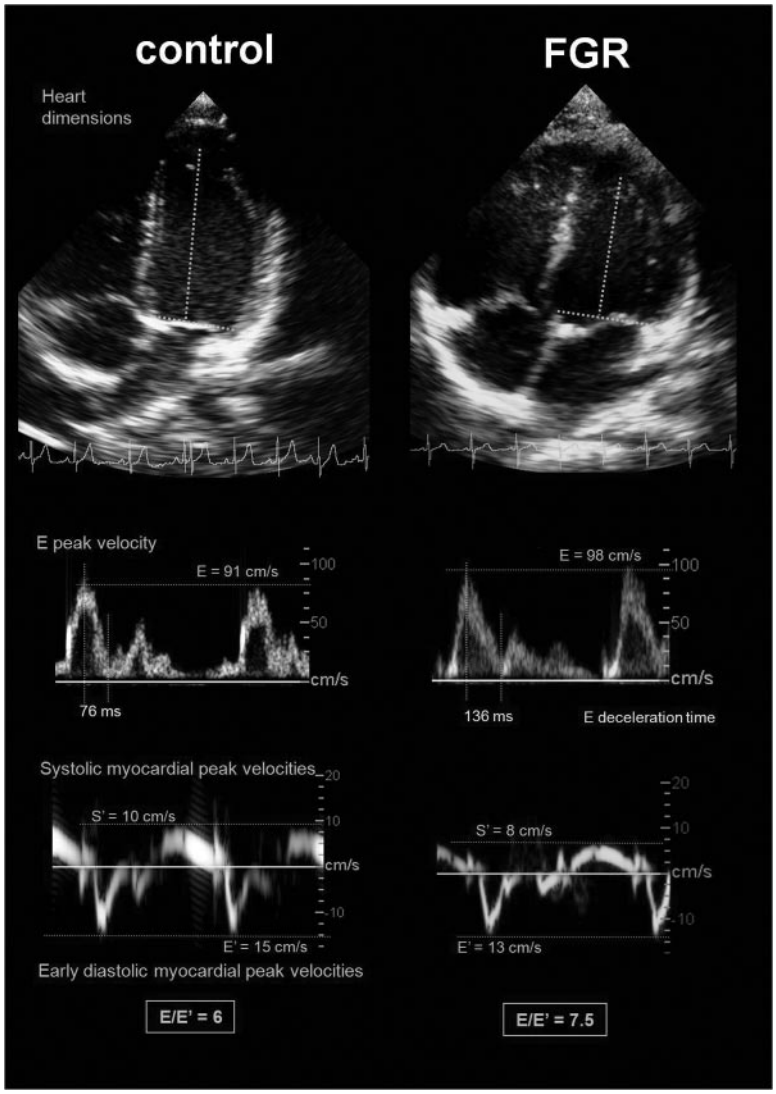

Figure 2. Echocardiographic images in a control subject and an FGR case subject. Top, Two-dimensional apical 4-chamber views at end diastole illustrating the more globular cardiac shape in FGR and showing the left ventricular longitudinal and transverse diameter measurement. Bottom, Spectral and tissue Doppler waves illustrating the increase of mitral early diastolic (E) deceleration time and E/E′ ratio, as well as the decrease of early diastolic (E′) and systolic (S′) myocardial peak velocities in FGR compared with control subjects.

weight below the 10th percentile according to local standards[13] for whom full prenatal information was available, including umbilical artery Doppler. For the purposes of the present study, FGR was classified as mild when umbilical artery Doppler was normal (pulsatility index <2 SDs) and severe FGR when it was abnormal (pulsatility index ≥2 SDs).[5] From the eligible population of 837 fetuses with growth restriction identified in fetal life and followed up into childhood, case subjects were randomly sampled and invited to participate in the study until a final study population of 40 case subjects with mild FGR and 40 with severe FGR was completed, in accordance with the sample-size requirements. A reference cohort of children born with a normal birth weight (>10th percentile) randomly sampled from pregnancies delivered at our institution were selected as a control group. Noneligibility criteria for control subjects were the same as for case subjects. Control subjects were matched 2-to-1 with mild FGR case subjects and 1-to-1 with severe FGR case subjects according to gender, birth date (±6 months), and gestational age at delivery (±1 week), calculated by first-trimester crown–rump length measurement. The study protocol was approved by the Hospital Clinic Ethics Committee, and written parental consent was obtained for all study participants. Figure 1 shows a flow diagram of the study population.

Study Protocol and Follow-Up

The study protocol consisted of a medical examination, echocardiography, and ultrasound carotid assessment. A blood sample extraction was also proposed, but if parents rejected it, the case subject was not excluded from the study. Anthropometric data, including each child's height, weight, and body mass index, were gathered at the time of the study examination, and their percentiles were calculated according to local reference values.

Cardiac Morphometry and Function

All echocardiographic examinations were performed according to a standardized protocol with a Siemens Sonoline Antares ultrasound system (Siemens Medical Systems, Malvern, Pa) with a 2- to 10-MHz phased-array transducer. An ECG was registered continuously during echocardiography. A complete 2-dimensional, M-mode, and Doppler echocardiographic examination was performed initially to assess structural heart integrity and morphometry. Linear measurements of base-to-apex length and basal diameter of left and right ventricles were determined from 2-dimensional images from an apical 4-chamber view at end diastole (Figure 2) according to a standardized protocol, and sphericity index was calculated as base-to-apex length/basal diameter.[14] Left ventricular end-diastolic septum and posterior wall thicknesses were measured by M-mode echocardiography from a parasternal long-axis view. Relative wall thickness was calculated as (posterior+septal wall thickness)/end-diastolic cavity diameter. Left ventricular ejection fraction (%) was obtained from 2-dimensional apical 4-chamber and 2-chamber views and calculated by Simpson's rule. Left cardiac output was calculated as follows: Cross-sectional aortic annulus area×aortic flow velocity

Table 1. Baseline Characteristics of the Study Groups

Characteristic	Controls (n=120)	Mild FGR (n=40)	Severe FGR (n=40)	Linear Tendency *P*
Male sex, %	46	40	38	0.560
White race, %	95	98	90	0.342
Low socioeconomic level, %	3	0	8	0.406
Familial early cardiovascular history, %†	17	10	27	0.121
Maternal characteristics				
Age, y	33±4	33±4	32±5	0.417
Height, cm	163±55	160±68*	162±74	0.209
Weight, kg	62±11	57±6*	65±12	0.313
BMI, kg/m^2	22 (21–25)	22 (20–24)	23 (21–27)	0.077
Smoking, cigarettes/d	0 (0–3)	0 (0–10)	0 (0–7)	0.904
Primiparity, %	64	73	70	0.539
Paternal characteristics				
Age, y	35±5	35±4	35±6	0.882
Height, cm	177±67	174±55	174±80	0.134
Weight, kg	79±11	77±11	79±12	0.668
BMI, kg/m^2	25 (24–27)	25 (24–27)	26 (24–28)	0.376
Smoking, cigarettes/d	0 (0–10)	0 (0–5)	4 (0–15)	0.011
Pregnancy complications				
In vitro fecundation	4	3	5	0.845
Preeclampsia	1	3	38*	<0.001
Gestational diabetes	3	15*	3	0.016
Prenatal glucocorticoid exposure				
Born preterm, %	85	‡	88	0.378
Born at term, %	0	0	‡	
Prenatal ultrasound				
Umbilical artery pulsatility index, *z* scores	0 (−1–1)	0 (−1–1)	6 (4–8)*	<0.001
Middle cerebral artery pulsatility index, *z* scores	0 (−1–1)	−1 (−1–1)*	−3 (−3–−2)*	<0.001
Ductus venosus pulsatility index, *z* scores	0 (−1–1)	−1 (−1–0)	1 (0–2)	0.241
Gestational age at delivery, wk	38 (34–40)	40 (39–40)*	32 (30–34)*	<0.001
Birth weight, g	3150 (2300–3550)	2630 (2505–2738)*	1065 (875–1402)*	<0.001
Birth weight percentile	55 (31–81)	3 (1–3)*	0 (0–0)*	<0.001
Umbilical artery pH	7.30 (7.25–7.35)	7.24 (7.17–7.28)*	7.24 (7.17–7.27)*	0.002
Days in neonatal intensive care unit	0 (0–5)	0 (0–3)	30 (27–60)*	<0.001
Major neonatal morbidity, %§	7	0	34*	<0.001
Breastfeeding, mo	4 (2–8)	5 (2–11)	4 (4–6)	0.927
Postnatal corticoid exposure, %	4	8	8	0.585
Postnatal growth hormone treatment, %	0	0	3	0.997

BMI indicates body mass index.

Data are mean±SD or median (interquartile range).

*$P<0.05$ compared with controls, calculated by linear or logistic regression.

†Defined as early cardiovascular disease (including congenital heart disease, coronary disease, hypertension, diabetes, or hypercholesterolemia) in expanded first-degree pedigree (male <55 years old; female <65 years old).

‡Not applicable (no mild cases born preterm or severe cases born at term).

§Major neonatal morbidity defined by the presence of bronchopulmonary dysplasia, necrotizing enterocolitis, intraventricular hemorrhage, periventricular leukomalacia, retinopathy, persistent ductus arteriosus, or sepsis.

integral×heart rate per minute. The internal diameter of the aortic annulus (with open valve) was measured from the 2-dimensional image in the parasternal long-axis view. The ascending aortic flow-velocity integral was measured with pulsed Doppler from an apical 5-chamber view. Peak early (E) and late (A) transvalvular filling velocities, E/A ratio, and deceleration time of E velocity were measured from mitral and tricuspid inflow velocities from an apical 4-chamber view. Isovolumic left ventricular relaxation time was measured from the end of the aortic wave to the beginning of the mitral early-filling wave. Mitral and tricuspid longitudinal motion was assessed by M-mode echocardiography from an apical 4-chamber view. Tissue Doppler imaging was applied in the spectral Doppler mode to record systolic (S′) and early diastolic (E′) peak myocardial velocities at the mitral lateral and septal annulus and the tricuspid lateral annulus from an apical 4-chamber view and measured in real time during the echocardiographic study. Mitral lateral

Table 2. Follow-Up Characteristics of the Study Groups

Characteristic	Controls (n=120)	Mild FGR (n=40)	Severe FGR (n=40)	Linear Tendency *P*
Age, y†	4.5 (2.6–5.6)	4.6 (3.4–4.9)	4.1 (2–4.7)	0.654
Anthropometric data				
Height, cm	109 (88–117)	105 (96–110)	94 (80–107)*	0.002
Height percentiles	52 (48–56)	50 (47–52)	48 (43–51)*	0.001
Weight, kg	18 (13–22)	16 (14–19)*	14 (11–18)*	0.369
Weight percentiles	49 (30–73)	37 (14–62)*	24 (9–47)*	0.212
Body mass index, kg/m^2	16 (15–17)	15 (15–17)*	16 (15–17)	0.480
Obesity, %‡	5	0	5	0.352

BMI indicates body mass index.

Data are median (interquartile range).

*$P<0.05$ compared with controls, calculated by linear or logistic regression adjusted for gender, age, gestational age at delivery, body surface area, heart rate, and association with preeclampsia or gestational diabetes.

†Children's age is corrected by gestational age at delivery.

‡Obesity defined as body mass index above 95th percentile for age and gender.

and septal E/E′ ratios were measured as described previously.[15] When blood was available, B-type natriuretic peptide concentrations were measured with the Siemens ADVIA Centaur B-type natriuretic peptide assay.

Vascular Assessment

Systolic and diastolic blood pressures were obtained at the beginning of the medical evaluation by a trained nurse while the child was seated after having rested for 5 to 10 minutes. Right and left carotid arteries were scanned according to a standardized protocol with a 13-MHz linear-array transducer. Longitudinal clips of the far wall of both carotid arteries were obtained approximately 1 cm proximal to the bifurcation, with the ECG recorded continuously. Carotid intima-media thickness (cIMT) measurements were performed offline based on a trace method with the assistance of a computerized program (Siemens Syngo Arterial Health Package). To obtain cIMT, 2 end-diastolic frames were selected and analyzed for mean intima-media thickness and diameter, and the average reading from these 2 frames was calculated for both right and left carotid arteries. Circumferential wall stress was calculated as follows: (Mean blood pressure×mean diastolic carotid diameter)/2×cIMT.

Statistical Analysis

The primary outcomes were cardiac dimensions and function. E/E′ ratio and S′ were used to calculate sample size because of the high reported sensitivity to detect preclinical cardiac dysfunction in children.[16–19] The sample size was calculated to enable us to observe a difference of 20% in E/E′ and S′ between the group of case subjects with severe FGR and control subjects, with 85% power and a 5% type I risk. Basal mean and within-group standard deviations were estimated according to published normative data in children,[18,19] which resulted in a required sample of 40 individuals in each group for E/E′ and 25 for S′. Conservatively, a sample size of 40 individuals in each group was designed. Data are presented as mean±SD, median (interquartile range), or percentages, as appropriate. Paired comparisons between the study and control groups were adjusted for age, gender, gestational age at delivery, body surface area, heart rate, and the presence of preeclampsia or gestational diabetes by linear (general linear model) or logistic regression analysis. In addition, a linear polynomial orthogonal contrast was also constructed for each model to test the hypothesis of a linear association across FGR-severity groups. Children were categorized into groups of control subjects, mild FGR, and severe FGR. All reported *P* values are 2-sided. The software statistical package SPSS 15.0 (SPSS, Chicago, Ill) was used for the statistical analysis.

Results

Anthropometric, echocardiographic, and vascular data were obtained from all patients included in the study. Parents agreed to permit blood sampling in 42.5% of controls, 55% of those with mild FGR, and 82.5% of those with severe FGR.

Baseline and Follow-Up Characteristics

Baseline characteristics are shown in Table 1. The study groups were similar in terms of maternal, paternal, and familial characteristics, with the exception of shorter parental height in children with mild FGR than in control subjects. As expected, mothers of FGR children had a greater occurrence of pregnancy complications, and these children had worse prenatal Doppler ultrasound findings, worse umbilical artery pH, and longer admittance in a neonatal intensive care unit.

Follow-up characteristics at the time the children were assessed are shown in Table 2. The age range was 2 to 6 years. At the time of evaluation, FGR children showed a linear tendency to lower height and weight values, with similar results for body mass index, compared with control subjects. All case subjects were asymptomatic, and none of them received treatment with diuretics.

Cardiac Morphometry and Function

Results of cardiac morphometry and function studies are shown in Table 3 and Figures 2 and 3. Cardiac shape was altered significantly, with the left and right sphericity indexes decreased significantly in children with mild and severe FGR. Interventricular septum, left posterior wall thickness, and relative wall thickness showed similar values in all study groups.

Although left ventricular ejection fraction and B-type natriuretic peptide were similar among the study groups, stroke volume was changed significantly, which was compensated for by a significantly increased heart rate to maintain output in children with severe FGR, with a significant tendency for decreased stroke volume and increased heart rate across FGR-severity groups. Systolic mitral and tricuspid ring displacements were decreased significantly in mild and severe FGR case subjects compared with control subjects. Children with severe FGR showed significantly lower longitudinal S′ in mitral lateral, mitral septal, and tricuspid annulus

Table 3. Cardiac Outcome of Study Groups

Characteristic	Controls (n=120)	Mild FGR (n=40)	Severe FGR (n=40)	Linear Tendency *P*
Cardiac morphometry†				
Left ventricle				
Base-to-apex length, mm	49 (34–63)	43 (33–53)*	40 (27–50)*	<0.001
Basal diameter, mm	26 (19–40)	30 (26–38)*	30 (22–37)*	<0.001
Sphericity index	1.8 (1.3–2.3)	1.4 (1.1–1.7)*	1.3 (1.1–1.7)*	<0.001
Interventricular septum, mm	6.8 (6.1–7.9)	6.7 (5.8–7.3)	6.4 (5.8–6.4)	0.352
Left posterior wall, mm	6.7 (6.1–7.3)	6.7 (5.8–7.5)	6.4 (5.9–6.9)	0.449
Relative wall thickness	0.40 (0.35–0.46)	0.40 (0.36–0.46)	0.40 (0.35–0.49)	0.832
Right ventricle				
Base-to-apex length, mm	39 (25–53)	35 (28–49)*	34 (22–45)	0.557
Basal diameter, mm	25 (16–33)	26 (20–33)*	25 (17–33)*	<0.001
Sphericity index	1.6 (1.2–2.4)	1.4 (1.1–1.9)*	1.4 (0.9–1.8)*	<0.001
Cardiac function				
Systolic function				
Left stroke volume, mL	28 (13–52)	30 (18–47)	22 (11–43)*	0.003
Heart rate, bpm	94 (67–178)	101 (79–127)	112 (81–180)*	0.026
Left cardiac output, L/min	2.6 (2.3–3.2)	3.1 (2.8–3.7)*	2.7 (2–2.9)*	0.004
Left ejection fraction, %	69 (50–88)	70 (56–87)	72 (59–91)	0.916
Mitral ring displacement, mm	12.5 (10.8–14.3)	9.6 (8.4–10.6)*	9.1 (8.2–10.7)*	<0.001
Tricuspid ring displacement, mm	16.9 (15–18.9)	15.8 (13.6–17.4)*	11.6 (10.6–13.4)*	<0.001
Mitral lateral S′, cm/s	10 (8–17)	9 (8–15)	9 (6–13)*	<0.001
Mitral septal S′, cm/s	10 (7–15)	9 (8–12)*	9 (7–11)*	<0.001
Tricuspid S′, cm/s	15 (11–21)	15 (12–24)	14 (10–19)*	0.033
Diastolic function				
Mitral E wave, cm/s	101 (98–11)	103 (97–11)	105 (93–11)	0.638
Mitral A wave, cm/s	62 (61–76)	60 (51–66)	70 (56–71)	0.526
Mitral E/A ratio	1.7 (1.1–2.9)	1.7 (1.2–2.4)	1.5 (1.1–2.7)	0.505
Tricuspid E wave, cm/s	67 (61–79)	64 (60–71)	70 (59–72)*	0.013
Tricuspid A wave, cm/s	47 (42–58)	44 (39–52)	49 (42–53)	0.247
Tricuspid E/A ratio	1.4 (1–3.5)	1.5 (0.9–2.2)	1.3 (1–2.2)	0.348
Left isovolumic relaxation time, ms	56 (40–80)	60 (40–88)	56 (40–76)	0.855
Mitral E deceleration time, ms	88 (52–128)	96 (56–148)*	100 (56–160)*	<0.001
Tricuspid E deceleration time, ms	107 (56–160)	105 (64–156)	115 (52–160)*	0.001
Mitral lateral E′, cm/s	19 (12–28)	18 (13–23)	16 (10–24)*	0.004
Mitral septal E′, cm/s	15 (11–19)	15 (12–18)	14 (11–24)*	0.001
Tricuspid E′, cm/s	20 (11–29)	19 (11–23)	18 (14–26)*	0.001
E/E′ (lateral)	5.4 (3.9–8.3)	5.6 (3.3–8.5)	6.3 (4.1–10.8)*	0.001
E/E′ (septal)	6.7 (4.7–9.4)	6.8 (3.7–9.4)	7.4 (4.5–10.2)*	0.001
B-type natriuretic peptide, pg/mL	12 (0–63)	12 (0–39)	13 (0–41)	0.730

Data are median (interquartile range).

*$P<0.05$ compared with controls, calculated by linear or logistic regression adjusted for gender, age, gestational age at delivery, body surface area, heart rate, and association with preeclampsia or gestational diabetes.

†Cardiac morphometry results measured in end diastole.

than control subjects, with a significant linear tendency to lower values across FGR-severity stages.

Although mitral and tricuspid E/A ratios and isovolumic left ventricular relaxation time were similar among study groups, mitral E deceleration time was increased significantly in mild and severe FGR with respect to control subjects. Tricuspid E deceleration time was increased significantly in children with severe FGR, although there was a significant linear tendency for an increase across severity groups. Children with severe FGR showed significantly lower longitudinal E′ in mitral lateral, mitral septal, and tricuspid annulus than control subjects, with a significant linear tendency to lower values across FGR-severity stages. Mitral lateral and septal E/E′ ratios were significantly higher in children with severe FGR than in control subjects, with a significant linear trend to higher values across severity stages.

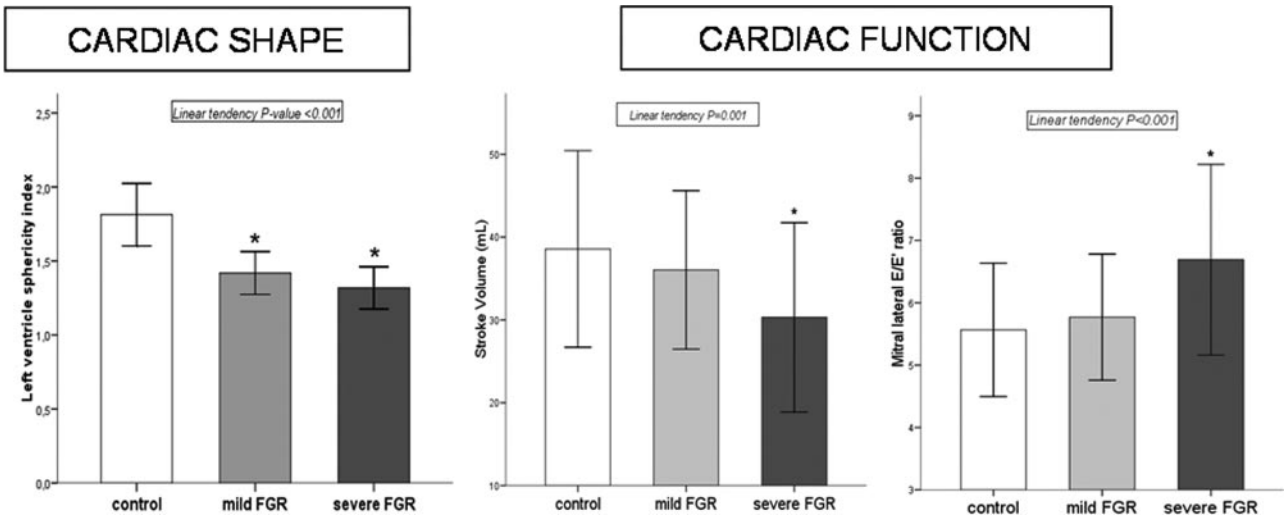

Figure 3. Results for left ventricle (LV) sphericity index, left stroke volume, and mitral annular E/E′ ratio in control subjects and subjects with FGR. Data are mean±SD. *$P<0.05$ compared with control subjects.

Vascular Assessment

Results of vascular assessment are displayed in Table 4 and Figure 4. Systolic and diastolic blood pressures were significantly higher in the mild and severe FGR groups. cIMT was increased significantly in children with severe FGR, even after adjustment for systolic blood pressure (linear tendency $P<0.001$; linear regression comparing control subjects and children with severe FGR $P<0.001$). Circumferential wall stress values were significantly higher in both the mild and severe FGR groups. There was a significant linear trend for higher values in relation to severity of FGR for all parameters evaluated.

Discussion

The present study provides direct clinical evidence that children with FGR show changes in cardiac morphology, subclinical cardiac longitudinal dysfunction, and arterial remodeling, all of which increase linearly with the severity of growth restriction. The findings support the existence of direct cardiac programming in FGR and suggest a new mechanistic pathway for the association between fetal growth and cardiovascular disease. The most striking finding was that children with FGR have a distinct cardiac geometry and shape, with less elongated and more globular ventricles. Morphometric measurements confirmed quantitatively an overall increase in transverse cardiac diameters, which led to apparent dilatation of the ventricular cavities. The data are in line with postmortem studies in human FGR that described hypoplasia in myocardial fibers.[20] These findings are also in agreement with our recent animal studies that showed the persistence of dilated cardiomyopathy–like features in utero into adulthood in a chick model of FGR under chronic hypoxia.[12]

The globular cardiac shape observed in children with FGR is most likely the result of changes in cardiac development induced by the working conditions of the fetal heart. The intrauterine state of chronic hypoxia and undernutrition,[21] together with increased placental vascular resistance,[22] results in a combined pressure and possibly volume overload of the fetal heart,[22,23] which induces abnormal cardiac function.[8,9,22] The resulting increased wall stress on the developing myocardial fibers should trigger a cardiac remodeling response to compensate for local stress. In normal conditions, acquired mild pressure overload leads to hypertrophy in the region of highest stress[24]; however, in the developing heart under conditions of sustained hypoxia and undernutrition, the myocardium might be unable to develop hypertrophic changes. Consequently, increased wall stress can only be compensated for by an increase in the local radius of curvature, which results in dilated changes and a more spherical cavity.

Therefore, as observed in the present study, children who were exposed to FGR will have intrinsically differently shaped hearts. It is likely that this is accompanied by stabilized changes in muscle fiber architecture,[25] because myocardial shape and fiber orientation are determined by stress and strain conditions.[26,27] A more globular ventricle,

Table 4. Vascular Outcome of Study Groups

Characteristic	Controls (n=120)	Mild FGR (n=40)	Severe FGR (n=40)	Linear Tendency *P*
Systolic blood pressure, mm Hg	100 (80–130)	105 (90–115)*	110 (90–120)*	0.019
Diastolic blood pressure, mm Hg	65 (45–90)	70 (57–85)*	70 (60–85)*	<0.001
cIMT, mm	0.37 (0.29–0.47)	0.38 (0.32–0.43)	0.41 (0.37–0.44)*	<0.001
Circumferential wall stress, mm Hg	72 (29–120)	78 (61–109)*	84 (58–102)*	<0.001

Data are median (interquartile range).

*$P<0.05$ compared with controls, calculated by linear or logistic regression adjusted for gender, age, gestational age at delivery, body surface area, heart rate, and association with preeclampsia or gestational diabetes.

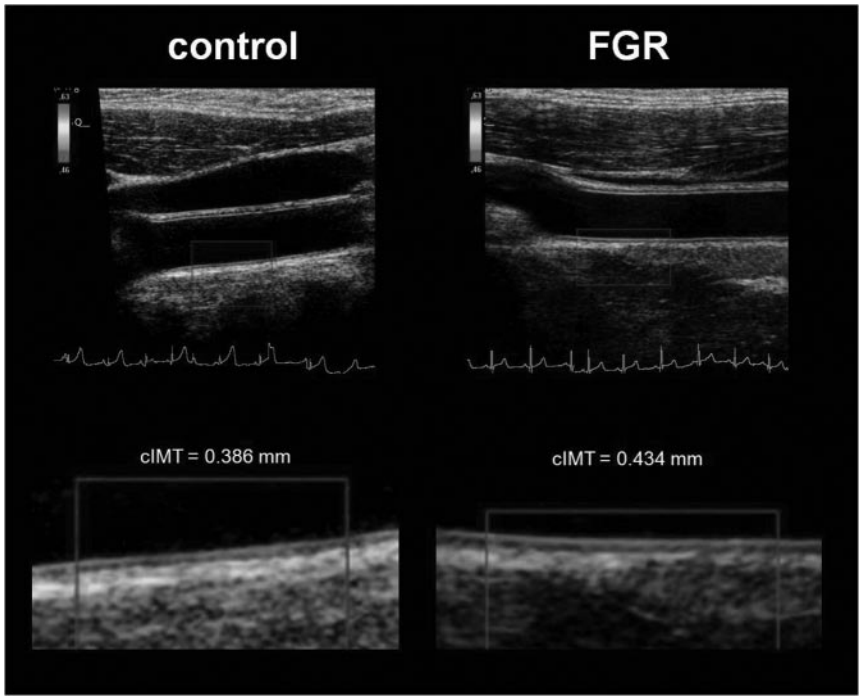

Figure 4. Ultrasound carotid images in a control subject and a case subject with FGR illustrating the increase of cIMT in FGR compared with control.

with potentially a different architecture, is not as efficient in generating the normal stroke volume,[28] which results in the need for an increased heart rate to maintain cardiac output, as observed in the present study. Because diastolic function depends on ventricular shape and torsion, as generated by the normal fiber architecture,[29] it was not unexpected that additional changes in diastolic parameters were found. Cardiac remodeling observed in FGR children in the present study might explain the increased risk of cardiovascular disease described in epidemiological studies on FGR.[3] Although the remodeled ventricles could compensate for their lower efficiency in childhood, any additional changes in their working conditions (eg, hypertension, ischemia, or arrhythmias) at a later age would result in an abnormally high increase in local wall stress and dilatation, because further shape adaptation of the ventricle is not possible.

The present study confirms and extends previous findings documenting a significantly increased carotid wall thickness[11] in children with FGR. Increased cIMT had been reported previously in newborns with FGR,[11] and the present results demonstrate that these changes persist into childhood. The increased arterial wall thickness is most likely the result of the overall pressure and possibly volume overload in the fetal circulation, in which vascular wall stress induces hypertrophy of the intima-media layer. In childhood, the remodeled arteries, now working under normal loading conditions, will produce an increased peripheral resistance and an elevation in blood pressure, which may contribute to increased cIMT.[30] Both elevated blood pressure and cIMT are additional accepted risk factors for future cardiovascular disease. However, because the hearts of FGR children did not demonstrate the hypertrophic changes characteristic of hypertensive cardiomyopathy, the cardiac changes in children with FGR are primary and not secondary.

There are several limitations and considerations of the present study. Because of the observed cardiac shape change in FGR, some of the echocardiographic measurements based on geometric assumptions such as the Simpson rule should be interpreted cautiously. The changes reported here are subclinical, and the long-term association with adult cardiovascular function and disease remains to be further proven. Furthermore, although the effect of prematurity and consequently of severe neonatal morbidity was accounted for in the study design, we cannot completely rule out the possibility that changes in FGR children could be a consequence of a more morbid neonatal course that results in cardiovascular stress.

The study was not designed to assess the effect of other factors on cardiovascular function. In the present study, cardiac changes were independent of obesity or an abnormal lipid profile, but the prevalence of these risk factors was very low in the present setting (online-only Data Supplement). The existence of metabolic programming in FGR is well demonstrated,[6] and the potential interactions between metabolic and cardiac programming in the risk of cardiovascular disease in these patients remains to be elucidated. The impact of gender was also addressed, and cardiovascular differences were equally observed in males and females (online-only Data Supplement), but we acknowledge that we may have lacked statistical power to detect subtle gender-associated differences. FGR children born preterm were compared with case subjects born at similar gestational age. The present findings are in line with recent studies that suggest that prematurity is not associated with fetal cardiovascular programming.[4] We acknowledge that the pooling of control subjects regardless of gestational age might be regarded as a potential limitation; however, term and preterm control subjects showed similar results (online-only Data Supplement), and all comparisons were adjusted by gestational age at delivery.

Exposure to prenatal glucocorticoids was also similar, and in addition, the influence of corticoids in cardiac function has been discounted recently in a large cohort study.[31] Even though approximately half of the severe cases of FGR were associated with preeclampsia, it has been reported recently that the presence of preeclampsia does not influence fetal cardiac function in severe FGR[32]; however, we acknowledge that the association with preeclampsia could in some cases be a form of familial predisposition. Consequently, analyses were adjusted by potential confounders such as body surface area, heart rate, or association with preeclampsia or gestational diabetes. Finally, other potential confounders such as socioeconomic status, race, familial early cardiovascular history, breastfeeding, parity, and parental smoking were similar among study groups.

In summary, the present study provides evidence of an association between FGR and cardiac remodeling and longitudinal dysfunction in childhood that shows a linear increase with the severity of growth restriction and is independent of gestational age at delivery, lipid profile, or body mass index. The importance of early identification and intervention in pediatric risk factors for cardiovascular disease is now well recognized[33]; however, FGR is not listed among the conditions presumed to increase cardiovascular risk in current consensus guidelines.[33] FGR affects 5% to 10% of all newborns, and therefore, the findings of the present study concern thousands of children each year. Primary cardiac programming might be one of the causes of increased cardiovascular mortality in adults born with FGR, and this may open new opportunities for monitoring and intervention in newborns and children affected with this condition. The present study identifies several therapeutic targets that could be used in future clinical trials. If these findings are confirmed, the impact of strategies[33–35] with beneficial effects on cardiac remodeling should be explored in FGR children.

Acknowledgments

We thank the study participants and their parents for their personal time and commitment to this project.

Sources of Funding

This study was supported by grants from the Fondo de Investigación Sanitaria (PI/060347; Spain), Ministerio de Ciencia e Innovación (SAF2009-08815; Spain), Centro para el Desarrollo Técnico Industrial (CENIT 20092012, apoyado por el Ministerio de Ciencia e Innovación, y Fondo de inversión local para el empleo; Spain), Cerebra Foundation for the Brain Injured Child (Carmarthen, Wales, United Kingdom), Thrasher Research Fund (Salt Lake City, Utah), Medical Research Council (GO601295 and MRC G0700288), and British Heart Foundation support (BHF Programme Grant RG/09/001/25940). Dr Crispi (CM07/00076) and Dr Eixarch (CM08/00105) are supported by a grant from the Carlos III Institute of Health (Spain).

Disclosures

None.

References

1. Berenson GS. Childhood risk factors predict adult risk associated with subclinical cardiovascular disease: the Bogalusa Heart Study. *Am J Cardiol*. 2002;90:3L–7L.
2. Zieske AW, Malcom GT, Strong JP. Natural history and risk factors of atherosclerosis in children and youth: the PDAY study. *Pediatr Pathol Mol Med*. 2002;21:213–237.
3. Barker DJ, Osmond C, Golding J, Kuh D, Wadsworth M. Growth in utero, blood pressure in childhood and adult life, and mortality from cardiovascular disease. *BMJ*. 1989;298:564–567.
4. Kaijser M, Bonamy AK, Akre O, Cnattingius S, Granath F, Norman M, Ekbom A. Perinatal risk factors for ischemic heart disease: disentangling the roles of birth weight and preterm birth. *Circulation*. 2008;117:405–410.
5. Figueras F, Eixarch E, Gratacos E, Gardosi J. Predictiveness of antenatal umbilical artery Doppler for adverse pregnancy outcome in small-for-gestational-age babies according to customised birthweight centiles: population-based study. *BJOG*. 2008;115:590–594.
6. Palinski W, Napoli C. Impaired fetal growth, cardiovascular disease, and the need to move on. *Circulation*. 2008;117:341–343.
7. Bozynski ME, Hanafy FH, Hernandez RJ. Association of increased cardiothoracic ratio and intrauterine growth retardation. *Am J Perinatol*. 1991;8:28–30.
8. Girsen A, Ala-Kopsala M, Makikallio K, Vuolteenaho O, Rasanen J. Cardiovascular hemodynamics and umbilical artery N-terminal peptide of proB-type natriuretic peptide in human fetuses with growth restriction. *Ultrasound Obstet Gynecol*. 2007;29:296–303.
9. Crispi F, Hernandez-Andrade E, Pelsers MM, Plasencia W, Benavides-Serralde JA, Eixarch E, Le Noble F, Ahmed A, Glatz JF, Nicolaides KH, Gratacos E. Cardiac dysfunction and cell damage across clinical stages of severity in growth-restricted fetuses. *Am J Obstet Gynecol*. 2008;199:254.e1–254.e4.
10. Leipala JA, Boldt T, Turpeinen U, Vuolteenaho O, Fellman V. Cardiac hypertrophy and altered hemodynamic adaptation in growth-restricted preterm children. *Pediatr Res*. 2003;53:989–993.
11. Skilton MK, Evans N, Griffiths KA, Harmer JA, Celermajer D. Aortic wall thickness in newborns with intrauterine restriction. *Lancet*. 2005;23:1484–1486.
12. Tintu A, Rouwet E, Verlohren S, Brinkmann J, Ahmad S, Crispi F, van Bilsen M, Carmeliet P, Staff AC, Tjwa M, Cetin I, Gratacos E, Hernandez-Andrade E, Hofstra L, Jacobs M, Lamers WH, Morano I, Safak E, Ahmed A, le Noble F. Hypoxia induces dilated cardiomyopathy in the chick embryo: mechanism, intervention, and long-term consequences. *PLoS ONE*. 2009;4:e5155.
13. Figueras F, Meler E, Iraola A, Eixarch E, Coll O, Figueras J, Francis A, Gratacos E, Gardosi J. Customized birthweight standards for a Spanish population. *Eur J Obstet Gynecol Reprod Biol*. 2008;136:20–24.
14. Lowes BD, Gill EA, Abraham WT, Larrain JR, Robertson AD, Bristow MR, Gilbert EM. Effects of carvedilol on left ventricular mass, chamber geometry, and mitral regurgitation in chronic heart failure. *Am J Cardiol*. 1999;83:1201–1205.
15. Nagueh SF, Middleton KJ, Kopelen HA, Zoghbi WA, Quiñones MA. Doppler tissue imaging: a noninvasive technique for evaluation of left ventricular relaxation and estimation of filling pressures. *J Am Coll Cardiol*. 1997;30:1527–1533.
16. Karakurt C, Koçcak G, Ozgen U. Evaluation of the left ventricular function with tissue tracking and tissue Doppler echocardiography in pediatric malignancy survivors after anthracycline therapy. *Echocardiography*. 2008;25:880–887.
17. Backer J, Matthys D, Gillebert TC, De Paepe A, De Sutter J. The use of tissue Doppler imaging for the assessment of changes in myocardial structure and function in inherited cardiomyopathies. *Eur J Echocardiogr*. 2005;6:243–250.
18. Uçcar T, Tutar E, Yalçcinkaya F, Cakar N, Ozçcakar ZB, Atalay S, Uncu N, Kara N, Ekim M. Global left-ventricular function by tissue Doppler imaging in pediatric dialysis patients. *Pediatr Nephrol*. 2008;23:779–785.
19. Zilberman MV, Du W, Das S, Sarnaik SA. Evaluation of left ventricular diastolic function in pediatric sickle cell disease patients. *Am J Hematol*. 2007;82:433–438.
20. Takahashi N, Nishida H, Arai T, Kaneda Y. Abnormal cardiac histology in severe intrauterine growth retardation infants. *Acta Paediatr Jpn*. 1995;37:341–346.
21. Soothill PW, Nicolides KH, Campbell S. Prenatal asphyxia, hyperlacticaemia, hypoglycaemia, and erythroblastosis in growth retarded fetuses. *BMJ*. 1987;294:1051–1053.
22. Verburg BO, Jaddoe VW, Wladimiroff JW, Hofman A, Witteman JC, Steegers EA. Fetal hemodynamic adaptive changes related to intrauterine growth: the Generation R Study. *Circulation*. 2008;117:649–659.
23. Gardiner H, Brodszki J, Marsal K. Ventriculovascular physiology of the growth-restricted fetus. *Ultrasound Obstet Gynecol*. 2001;18:47–53.

24. Baltabaeva A, Marciniak M, Bijnens B, Moggridge J, He FJ, Antonios TF, MacGregor GA, Sutherland GR. Regional left ventricular deformation and geometry analysis provides insights in myocardial remodeling in mild to moderate hypertension. *Eur J Echocardiogr*. 2008;9:501–508.
25. Greenbaum RA, Ho SY, Gibson DG, Becker AE, Anderson RH. Left ventricular fibre architecture in man. *Br Heart J*. 1981;45:248–263.
26. Taber LA. Mechanical aspects of cardiac development. *Prog Biophys Mol Biol*. 1998;69:237–255.
27. Arts T, Prinzen FW, Snoeckx LH, Rijcken JM, Reneman RS. Adaptation of cardiac structure by mechanical feedback in the environment of the cell: a model study. *Biophys J*. 1994;66:953–961.
28. Blyakhman FA, Shklyar TF, Pavlov IA, Sokolov SY, Grinko AA. Why the left ventricle is not a sphere. *Appl Bionics Biomech*. 2004;1:101–105.
29. Notomi Y, Popovic ZB, Yamada H, Wallick DW, Martin MG, Oryszak SJ, Shiota T, Greenberg NL, Thomas JD. Ventricular untwisting: a temporal link between left ventricular relaxation and suction. *Am J Physiol Heart Circ Physiol*. 2008;294:H505–H513.
30. Mzayek F, Hassig S, Sherwin R, Hughes J, Chen W, Srinivasan S, Berenson G. The association of birth weight with developmental trends in blood pressure from childhood through mid-adulthood: the Bogalusa Heart study. *Am J Epidemiol*. 2007;166:413–420.
31. de Vries WB, Karemaker R, Mooy NF, Strengers JL, Kemperman H, Baerts W, Veen S, Visser GH, Heijnen CJ, van Bel F. Cardiovascular follow-up at school age after perinatal glucocorticoid exposure in prematurely born children: perinatal glucocorticoid therapy and cardiovascular follow-up. *Arch Pediatr Adolesc Med*. 2008;162:738–744.
32. Crispi F, Comas M, Hernandez-Andrade E, Eixarch E, Gomez O, Figueras F, Gratacós E. Does preeclampsia influence fetal cardiovascular function? *Ultrasound Obstet Gynecol*. 2009;34:660–665.
33. Kavey RE, Allada V, Daniels SR, Hayman LL, McCrindle BW, Newburger JW, Parekh RS, Steinberger J. Cardiovascular risk reduction in high-risk pediatric patients: a scientific statement from the American Heart Association Expert Panel on Population and Prevention Science; the Councils on Cardiovascular Disease in the Young, Epidemiology and Prevention, Nutrition, Physical Activity and Metabolism, High Blood Pressure Research, Cardiovascular Nursing, and the Kidney in Heart Disease; and the Interdisciplinary Working Group on Quality of Care and Outcomes Research: endorsed by the American Academy of Pediatrics. *Circulation*. 2006;114:2710–2738.
34. de Lorgeril M, Salen P, Martin JL, Monjaud I, Delaye J, Mamelle N. Mediterranean diet, traditional risk factors, and the rate of cardiovascular complications after myocardial infarction: final report of the Lyon Diet Heart Study. *Circulation*. 1999;99:779–785.
35. Meyer AA, Kundt G, Lenschow U, Schuff-Werner P, Kienast W. Improvement of early vascular changes and cardiovascular risk factors in obese children after a six-month exercise program. *J Am Coll Cardiol*. 2006;48:1865–1870.

CLINICAL PERSPECTIVE

The present study provides evidence that fetal growth restriction, a condition that affects 5% to 10% of all newborns, is associated with cardiac remodeling and longitudinal myocardial dysfunction in childhood. This association shows a linear increase with the severity of growth restriction and is independent of gestational age at delivery. From a pathophysiological perspective, the results of the study are relevant because they may help to clarify the long-described epidemiological relationship between fetal growth restriction and increased cardiovascular mortality in adulthood. This may result in new opportunities for monitoring and intervention beginning in early life. The present study identifies several therapeutic targets that might be used in future clinical trials. From a public health perspective, the study is relevant because the importance of early identification and intervention in pediatric risk factors for cardiovascular disease is now well recognized; however, fetal growth restriction is not listed among the cardiovascular risk factors in current consensus guidelines. Public health strategies focused at targeting infants affected by fetal growth restriction would involve thousands of children yearly and could reduce the cardiovascular risk of these children when they reach an elderly age.

Fetal growth restriction results in remodeled and less efficient hearts in children

Fàtima Crispi, Bart Bijnens, Francesc Figueras, Joaquim Bartrons, Elisenda Eixarch, Ferdinand Le Noble, Asif Ahmed, Eduard Gratacós.

SUPPLEMENTAL MATERIAL

Supplemental Methods

Study protocol and follow-up

Parents accepting to participate in the study were given an appointment for a single visit in which all examinations contemplated in the study were performed. The study protocol consisted in a medical examination and a dietary questionnaire. A blood sample extraction was also proposed but, if parents rejected it, the case was not excluded from the study. The study was completed by a detailed echocardiography and ultrasound carotid assessment. The follow-up team consisted of a research nurse trained to perform the medical evaluation (including height, weight and blood pressure), blood sample extraction and dietary questionnaire, and two experienced physicians (F.C., J.B.) who performed echocardiography and carotid assessment.

Perinatal, including fetal ultrasound and Doppler exams, demographic and neonatal data were already recorded in the database, but were confirmed by review of medical records and clinical databases and by parental interview at the time of study evaluation. Low socioeconomic class was defined as routine occupation, long-term unemployment or never worked, for both the pregnant woman and her partner, according to the UK National Statistics Socio-Economic Classification.[1] Familiar early cardiovascular history was defined as the presence of early cardiovascular disease (including congenital heart disease, coronary disease, hypertension, diabetes or hypercholesterolemia) in expanded first degree

pedigree (male<55 years; female <65 years). Preeclampsia was defined as blood pressure >140/90 mmHg on two occasions at least 4 h apart and proteinuria >300 mg/24 h.[2] Prenatal Doppler ultrasound examinations were performed by a Siemens Sonoline Antares (Siemens Medical Systems, Malvern, PA, USA) or a Voluson 730 Expert (GE Medical Systems, Milwaukee, WI, USA) with 6-4 MHz linear curved array probes. The examination included: umbilical artery pulsatility index calculated from three or more consecutive waveforms obtained from a free-floating portion of the umbilical cord during the absence of fetal movement, at insonation angles <30º; middle cerebral artery pulsatility index measured distally to the junction of the internal carotid artery in a transverse view of the fetal skull at the level of the circle of Willis; and ductus venosus pulsatility index measured either in a mid sagittal view of the fetal thorax or in a transversal plane through the upper abdomen prior to its entrance to the inferior vena cava, positioning the Doppler gate at the ductus venosus isthmic portion. All prenatal Doppler measurements were converted into Z-scores (standard deviations from the gestational age mean).[3-4] Major neonatal morbidity was defined by the presence of bronchopulmonary dysplasia, necrotizing enterocolitis, intraventricular hemorrhage, periventricular leukomalacia, retinopathy, persistent ductus arteriosus or sepsis. Anthropometric data including child's height, weight and body mass index were measured at the time of the study examination, and their percentiles were calculated according to local reference values.[5]

Two children were excluded because of structural heart defect (atrial septal defect and persistent ductus arteriosus) diagnosed at the time of the study and referred to the Department of Pediatric Cardiovascular Surgery of Hospital Sant Joan de Déu.

Children with hypertension (blood pressure above 95th percentile for age, gender and height), abnormal lipid profile or suboptimal nutritional status were referred to their pediatrician for follow-up and treatment.

Nutritional and lipid/glucose profile

Nutritional status was assessed by questionnaires in which parents reported the child's weighted food and beverages diaries consumed for 3 days. Nutrient analysis for such diet was performed with DietSource Junior 1.1.23 software provided by Nestle Healthcare Nutrition S.A. (Esplugues de Llobregat, Spain). Mean intakes of dietary energy, protein, carbohydrate, fat, and saturated, monounsaturated and polyunsaturated fatty acids were measured. Protein, carbohydrate and fat percentages were calculated from the total diet. Saturated monounsaturated and polyunsaturated fatty acids percentages were calculated from the total fat intake.

Total cholesterol, high-density lipoprotein, triglyceride, glucose and C-reactive protein concentrations were measured by standard methods on an automatic analyzer (Olympus AU-400, Germany) in fasting blood samples. Low-density lipoprotein concentrations were calculated according to the Friedewald formula.

Cardiac morphometry and function

All echocardiographic exams were performed following a standardized protocol[6-7] using a Siemens Sonoline Antares (Siemens Medical Systems, Malvern, PA, USA) with 2-10 MHz phased-array transducer. Children were studied when resting quietly or asleep. Electrocardiogram was registered continuously during echocardiography. All parameters were measured in 3 or 4 consecutive cardiac cycles and the average value was recorded.

Vascular assessment

Systolic and diastolic blood pressure was obtained at the beginning of the medical evaluation by a trained nurse while the child was sitting after resting 5 to 10 minutes. It was measured manually in the child's right arm and determined from appearance (Korotkoff sound phase 1) and disappearance (Korotkoff sound phase 5) of pulsations auscultated over the braquial artery. Different cuffs were used adjusting to one third size of child's arm. When blood pressure was considered elevated (>90th percentile according to standard reference values), a second measurement was performed and the lower measurement was recorded.

Right and left carotid arteries were scanned following a standardized protocol according to the American Society of Echocardiography[8] and American Heart Association guidelines.[9] This technique has been validated in children showing an acceptable inter- and intra-observer variability.[9-11] To determine carotid wall thickness reliability in our population, 50 children were evaluated by the same operator and 30 children by two independent operators.

Statistical analysis

The primary outcomes were cardiac dimensions and function. E/E' ratio and S' were used to calculate sample size because of the high reported sensitivity to detect preclinical cardiac dysfunction in children.[12-18] Increased E/E' has been reported as a marker of diastolic dysfunction in children with obesity and familial hypercholesterolemia,[12] exposure to chemotherapies with known cardiotoxic effects,[13] cardiomyopathy[14] and cardiac involvement in renal[15] and connective tissue diseases.[16] Moreover, S' has been demonstrated to precede clinical cardiac dysfunction in a substantial number of conditions, such as inherited cardiomyopathies,[14] anthracycline-induced cardiomyopathy,[17] mitral and aortic regurgitation[18] and cardiac involvement in connective tissue diseases.[16]

Supplemental Results

Nutritional and lipid/glucose profile

Nutritional parameters and lipid/glucose profile showed similar values among all study groups (Table 5).

Cardiac morphometry and function

Cardiovascular results in males and females are shown in Tables 6a and 6b. The data were analyzed separately for males and females, and similar results were found for both gender groups.

Table 7 shows cardiovascular results in term and preterm controls.

There was no significant correlation between longitudinal-transverse ratio and body surface area was measured in controls (R^2=0.029, *P value=0.771*). A significant positive correlation between longitudinal-transverse ratio and body surface area was measured in FGR cases (mild FGR: R^2=0.377, *P value=0.020;* R^2=0.505, *P value=0.001*).

Vascular assessment

Intraclass Correlation Coefficients for cIMT were 0.75 and 0.70 for intra- and inter- observer variability respectively.

Supplemental Tables

Table 5: Nutritional parameters and lipid/glucose profile of the study groups

Characteristic	controls (N=120)	mild FGR (N=40)	severe FGR (N=40)	Linear tendency P Value
Nutritional assessment	**(N=114)**	**(N=38)**	**(N=37)**	
Total energy (kcal)	1606±340	1522±374	1525±388	0.964
Proteins (%)	18±6	18±3	18±3	0.818
Carbohydrates (%)	48±9	49±7	49±7	0.645
Fats (%)	34±6	34±5	33±6	0.325
Saturated fatty acids (%)	38±7	38±7	40±7	0.415
Monounsaturated fatty acids (%)	34±6	36±5	34±5	0.198
Polyunsaturated fatty acids (%)	8±5	7±3	7±2	0.516
Lipid and glucose profile	**(N=51)**	**(N=22)**	**(N=33)**	
Total cholesterol (mg/dL)	160 [142,185]	174 [147,194]	168 [137,189]	0.811
High-density lipoproteins (mg/dL)	54 [41,61]	48 [40,60]	55 [41,60]	0.513
Low-density lipoproteins (mg/dL)	96 [75,114]	110 [79,128]	96 [71,109]	0.383
Triglyceride (mg/dL)	73 [59,98]	53 [43,110]	78 [63,110]	0.703
Glucose (mg/dL)	89 [82,95]	88 [84,92]	86 [84,92]	0.374
C-reactive protein (mg/dL)	0.75 [0,1]	1 [0,5]	0.30 [0,2]	0.797

Data are mean±SD or median [interquartile range].
FGR = fetal growth restriction.
* P-value<0.05 as compared to controls calculated by linear or logistic regression adjusted by gender, age, gestational age at delivery, body surface area, heart rate and association to preeclampsia or gestational diabetes.

Table 6a: Cardiac and vascular outcome of the males in the study groups

Characteristic	Controls (N=55)	mild FGR (N=16)	severe FGR (N=15)	Linear tendency P Value
Cardiac morphometry†				
Left ventricle				
Base-to-apex length (mm)	49 [45,54]	41 [39,45]*	40 [36,44]*	<0.001
Basal diameter (mm)	27 [24,30]	31 [29,32]*	30 [27,33]*	0.013
Longitudinal-transverse ratio	1.8 [1.7,1.9]	1.3 [1.3,1.4]*	1.3 [1.3,1.4]*	<0.001
Interventricular septum (mm)	7 [6,8]	7 [6,8]	6 [6,8]	0.033
Left posterior wall (mm)	7 [6,8]	7 [6,8]	6 [6,6]	0.008
Right ventricle				
Base-to-apex length (mm)	40 [36,44]	36 [32,41]*	34 [32,39]*	0.003
Basal diameter (mm)	25 [20,28]	26 [25,28]*	26 [21,27]*	0.465
Longitudinal-transverse ratio	1.7 [1.5,1.8]	1.4 [1.3,1.5]*	1.4 [1.3,1.6]*	<0.001
Cardiac function				
Systolic function				
Left stroke volume (mL)	29 [23,33]	27 [23,34]	23 [20,34]*	0.056
Heart rate (bpm)	95 [85,112]	99 [88,110]	106 [102,118]	0.045
Left ejection fraction (%)	69 [[2,72]	71 [67,74]	71 [66,74]	0.314
Mitral ring displacement (mm)	13 [10,15]	10 [9,11]*	9 [8,10]*	<0.001
Tricuspid ring displacement (mm)	17 [15,19]*	14 [13,16]*	11 [10,14]*	<0.001
Mitral annular S' (cm/s)	11 [9,12]	9 [9,10]*	8 [8,10]*	<0.001
Mitral septal S' (cm/s)	10 [9,10]	9 [9,10]	9 [9,9]*	0.026
Tricuspid S' (cm/s)	16 [14,17]	15 [14,17]	15 [14,15]	0.151
Diastolic function				
Mitral E/A ratio	1.7 [1.4,1.8]	1.6 [1.5,2]	1.5 [1.3,1.7]	0.596
Tricuspid E/A ratio	1.4 [1.2,1.6]	1.6 [1.4,1.7]	1.2 [1.1,1.6]	0.187
Left isovolumic relaxation time (ms)	56 [48,64]	52 [49,62]	56 [52,56]	0.897
Mitral E deceleration time (ms)	88 [76,96]	96 [76,114]*	96 [88,102]*	0.011
Tricuspid E deceleration time (ms)	104 [96,124]	112 [92,124]	120 [100,128]	0.186
Mitral annular E' (cm/s)	18 [17,21]	17 [17,20]	16 [14,18]*	0.002
Mitral septal E' (cm/s)	15 [14,16]	15 [14,16]	14 [13,15]*	0.008
Tricuspid E' (cm/s)	20 [19,21]	20 [19,21]	20 [19,20]	0.215
Annular E/E'	5.5 [4.6,6.2]	5.5 [5.2,6]	6.1 [5.6,8]*	0.001
Septal E/E'	6.9 [6.2,7.4]	6.9 [6.1,7.8]	7.3 [6.7,8.8]*	0.005
B-type natriuretic peptide (pg/mL)	11 [7,15]	13 [10,14]	13 [12,18]	0.678
Vascular assessment				
Systolic blood pressure (mmHg)	100 [98,110]	107 [105,113]	110 [105,110]*	0.041
Diastolic blood pressure (mmHg)	65 [60,70]	70 [65,75]*	70 [70,75]*	0.015
Carotid mean intima-media thickness (mm)	0.38 [0.36,0.40]	0.38 [0.36,0.40]	0.41 [0.40,0.42]*	0.001
Circumferential wall stress (mmHg)	77 [68,85]	83 [78,93]	95 [89,98]*	0.047

Data are median [interquartile range].
FGR = fetal growth restriction. BMI = body mass index.
* P-value<0.05 as compared to controls calculated by linear or logistic regression.
† Cardiac morphometry measured in end-diastole.

Table 6b: Cardiac and vascular outcome of the females in the study groups

Characteristic	Controls (N=65)	mild FGR (N=24)	severe FGR (N=25)	Linear tendency P Value
Cardiac morphometry†				
Left ventricle				
Base-to-apex length (mm)	48 [41,52]	45 [38,47]*	40 [32,43]*	<0.001
Basal diameter (mm)	26 [23,28]	30 [28,32]*	30 [27,31]*	<0.001
Longitudinal-transverse ratio	1.8 [1.7,2]	1.5 [1.3,1.6]*	1.3 [1.2,1.4]*	<0.001
Interventricular septum (mm)	7 [6,8]	7 [6,7]	6 [6,7]	0.089
Left posterior wall (mm)	6 [6,7]	6 [6,7]	6 [6,7]	0.324
Right ventricle				
Base-to-apex length (mm)	36 [31,42]	35 [32,39]	33 [28,37]	0.012
Basal diameter (mm)	24 [20,27]	26 [23,28]	24 [22,27]*	0.989
Longitudinal-transverse ratio	1.5 [1.4,1.7]	1.4 [1.3,1.5]*	1.3 [1.2,1.5]*	0.002
Cardiac function				
Systolic function				
Left stroke volume (mL)	28 [24,33]	27 [24,32]	19 [17,24]*	<0.001
Heart rate (bpm)	94 [90,107]	103 [90,108]	114 [104,122]	0.001
Left ejection fraction (%)	69 [64,73]	70 [66,74]	71 [67,77]	0.056
Mitral ring displacement (mm)	12 [11,13]	9 [8,10]*	10 [8,10]*	<0.001
Tricuspid ring displacement (mm)	17 [16,18]	16 [14,18]	12 [11,13]*	<0.001
Mitral annular S' (cm/s)	10 [9,11]	10 [9,11]	9 [8,11]*	0.011
Mitral septal S' (cm/s)	10 [9,10]	9 [8,10]	9 [8,9]*	0.002
Tricuspid S' (cm/s)	15 [14,17]	16 [14,17]	14 [13,15]*	0.006
Diastolic function				
Mitral E/A ratio	1.7 [1.3,19]	1.7 [1.6,1.9]	1.5 [1.3,1.7]	0.274
Tricuspid E/A ratio	1.4 [1.2,1.6]	1.4 [1.3,1.7]	1.4 [1.2,1.7]	0.651
Left isovolumic relaxation time (ms)	56 [52,64]	64 [54,64]	54 [48,58]	0.111
Mitral E deceleration time (ms)	88 [76,96]	96 [86,104]*	106 [92,114]*	<0.001
Tricuspid E deceleration time (ms)	108 [96,120]	100 [90,112]	114 [104,132]*	0.101
Mitral annular E' (cm/s)	18 [17,20]	19 [17,19]	16 [15,18]	0.004
Mitral septal E' (cm/s)	15 [14,17]	16 [15,17]	14 [13,15]	0.099
Tricuspid E' (cm/s)	19 [18,21]	19 [18,22]	18 [17,20]*	0.030
Annular E/E'	5.2 [4.9,6.4]	5.7 [5.3,6.3]	6.4 [5.6,7.7]*	<0.001
Septal E/E'	6.5 [5.8,7.4]	6.7 [5.9,7.4]	7.4 [6.9,7.9]*	0.005
B-type natriuretic peptide (pg/mL)	12 [8,22]	12 [6,13]	12 [7,23]	0.522
Vascular assessment				
Systolic blood pressure (mmHg)	100 [95,110]	105 [100,113]*	106 [100,110]	0.068
Diastolic blood pressure (mmHg)	65 [60,70]	70 [65,75]*	70 [65,70]*	0.002
Carotid mean intima-media thickness (mm)	0.37 [0.34,0.39]	0.38 [0.37,0.39]	0.40 [0.39,0.42]*	<0.001
Circumferential wall stress (mmHg)	70 [65,76]	75 [69,79]	76 [69,87]*	0.015

Data are median [interquartile range].
FGR = fetal growth restriction. BMI = body mass index.
* P-value<0.05 as compared to controls calculated by linear or logistic regression.
† Cardiac morphometry measured in end-diastole.

Table 7: Cardiac and vascular outcome of the term and preterm controls

Characteristic	Term controls (N=80)	Preterm controls (N=40)	P Value
Cardiac morphometry†			
Left ventricle			
Base-to-apex length (mm)	49 [46,54]	44 [41,49]	0.436
Basal diameter (mm)	28 [24,30]	25 [23,26]	0.123
Longitudinal-transverse ratio	1.80 [1.64,1.98]	1.84 [1.70,1.93]	0.461
Interventricular septum (mm)	6.8 [6.4,7.9]	6.7 [6.1,7.7]	0.786
Left posterior wall (mm)	6.8 [6.1,7.6]	6.4 [6.1,7]	0.382
Right ventricle			
Base-to-apex length (mm)	40 [35,44]	38 [32,41]	0.412
Basal diameter (mm)	26 [23,28]	23 [19,27]	0.056
Longitudinal-transverse ratio	1.58 [1.44,1.76]	1.66 [1.43,1.79]	0.351
Cardiac function			
Systolic function			
Left stroke volume (mL)	28 [23,32]	29 [22,36]	0.055
Heart rate (bpm)	93 [87,107]	102 [92,117]	0.412
Left ejection fraction (%)	68 [62,72]	71 [67,75]	0.230
Mitral ring displacement (mm)	12.9 [11.2,15.3]	11.6 [10.1,12.5]	0.060
Tricuspid ring displacement (mm)	17.7 [15.5,19.5]	15.7 [14.9,17]	0.182
Mitral annular S' (cm/s)	10 [9,11]	10 [9,11]	0.940
Mitral septal S' (cm/s)	10 [9,10]	10 [9,11]	0.747
Tricuspid S' (cm/s)	15 [14,17]	16 [14,16]	0.270
Diastolic function			
Mitral E/A ratio	1.68 [1.41,1.90]	1.56 [1.27,1.8]	0.833
Tricuspid E/A ratio	1.43 [1.22,1.63]	1.36 [1.16,1.56]	0.654
Left isovolumic relaxation time (ms)	56 [50,64]	56 [52,60]	0.876
Mitral E deceleration time (ms)	88 [80,100]	88 [72,92]	0.550
Tricuspid E deceleration time (ms)	108 [96,124]	104 [96,112]	0.387
Mitral annular E' (cm/s)	19 [17,21]	18 [17,19]	0.083
Mitral septal E' (cm/s)	15 [14,17]	16 [14,17]	0.396
Tricuspid E' (cm/s)	19 [18,21]	20 [19,22]	0.243
Annular E/E'	5.2 [4.6,6.3]	5.5 [4.9,6.4]	0.378
Septal E/E'	6.7 [6,7.5]	6.6 [5.8,7.2]	0.930
B-type natriuretic peptide (pg/mL)	10 [5,13]	13 [10,22]	0.899
Vascular assessment			
Systolic blood pressure (mmHg)	100 [95,110]	100 [100,110]	0.112
Diastolic blood pressure (mmHg)	60 [60,70]	65 [60,70]	0.250
Carotid mean intima-media thickness (mm)	0.37 [0.35,0.39]	0.38 [0.36,0.39]	0.642
Circumferential wall stress (mmHg)	73 [67,83]	71 [59,78]	0.311

Data are median [interquartile range].
BMI = body mass index.
* P-value<0.05 as compared to term controls calculated by linear or logistic regression.
† Cardiac morphometry measured in end-diastole.

Supplemental References

1. Rose D, Pevalin DJ (with O'Reilly K). The National Statistics Socioeconomic Classification: Origins, Development and Use. ONS: London, 2001.
2. Report of the National High Blood Pressure Education Program Working Group on High Blood Pressure in Pregnancy. Am J Obstet Gynecol 2000;183:S1-S22.
3. Baschat AA. Gembruch U. The cerebroplacental Doppler ratio revisited. Ultrasound Obstet Gynecol 2003;21:124-7.
4. Hecher K, Campbell S, Snijders R, Nicolaides K. Reference ranges for fetal venous and atrioventricular blood flow parameters. Ultrasound Obstet Gynecol. 1994;4:381-90.
5. Carrascosa A, Fernández JM, Fernández C, Ferrández A, López JP. Estudio transversal español de crecimiento 2008. Parte II: valores de talla, peso e índice de masa corporal desde el nacimiento hasta la talla adulta. An Pediatr (Barc) 2008;68:552-69.
6. Gottdiener JS, Bednarz J, Devereux R, Gardin J, Klein A, Manning WJ, Morehead A, Kitzman D, Oh J, Quinones M, Schiller NB, Stein JH, Weissman NJ; American Society of Echocardiography. American Society of Echocardiography recommendations for use of echocardiography in clinical trials. J Am Soc Echocardiogr. 2004;17:1086-119.
7. Lang RM, Bierig M, Devereux RB, Flachskampf FA, Foster E, Pellikka PA, Picard MH, Roman MJ, Seward J, Shanewise JS, Solomon SD, Spencer KT, Sutton MS, Stewart WJ; Chamber Quantification Writing Group; American Society of Echocardiography's Guidelines and Standards Committee; European Association of Echocardiography. Recommendations for chamber quantification: a report from the American Society of Echocardiography's Guidelines and Standards Committee and the Chamber Quantification Writing Group, developed in conjunction with the European Association of Echocardiography, a branch of the European Society of Cardiology. J Am Soc Echocardiogr. 2005;18:1440-63.
8. Stein JH, Korcarz CE, Hurst RT, Lonn E, Kendall CB, Mohler ER, Najjar SS, Rembold CM, Post WS; American Society of Echocardiography Carotid Intima-Media Thickness

Task Force. Use of carotid ultrasound to identify subclinical vascular disease and evaluate cardiovascular disease risk: a consensus statement from the American Society of Echocardiography Carotid Intima-Media Thickness Task Force. Endorsed by the Society for Vascular Medicine. American Society of Echocardiography Carotid Intima-Media Thickness Task Force. J Am Soc Echocardiogr. 2008;21:93-111.

9. Urbina EM, Williams RV, Alpert BS, Collins RT, Daniels SR, Hayman L, Jacobson M, Mahoney L, Mietus-Snyder M, Rocchini A, Steinberger J, McCrindle B; American Heart Association Atherosclerosis, Hypertension, and Obesity in Youth Committee of the Council on Cardiovascular Disease in the Young. Noninvasive assessment of subclinical atherosclerosis in children and adolescents: recommendations for standard assessment for clinical research: a scientific statement from the American Heart Association.Hypertension. 2009;54:919-50.
10. Pauciullo P, Iannuzzi A, Sartorio R, Irace C, Covetti G, Di Costanzo A, Rubba P. Increased intima-media thickness of the common carotid artery in hypercholesterolemic children. Arterioscler Thromb Vasc Biol 1994;14;1075-1079
11. Iannuzzi A, Licenziati MR, Acampora C, Salvatore V, Auriemma L, Romano ML, Panico S, Rubba P, Trevisan M. Increased carotid intima-media thickness and stiffness in obese children. Diabetes Care. 2004 Oct;27(10):2506-8.
12. Van Putte-Katier N, Rooman RP, Haas L, Verhulst SL, Desager KN, Ramet J, Suys BE. Early cardiac abnormalities in obese children: importance of obesity per se versus associated cardiovascular risk factors. Pediatr Res. 2008;64:205-9.
13. Karakurt C, Koçak G, Ozgen U. Evaluation of the left ventricular function with tissue tracking and tissue Doppler echocardiography in pediatric malignancy survivors after anthracycline therapy. Echocardiography. 2008;25:880-7.
14. De Backer J, Matthys D, Gillebert TC, De Paepe A, De Sutter J. The use of Tissue Doppler Imaging for the assessment of changes in myocardial structure and function in inherited cardiomyopathies. Eur J Echocardiogr. 2005;6:243-50.

15. Uçar T, Tutar E, Yalçinkaya F, Çakar N, Ozçakar ZB, Atalay S, Uncu N, Kara N, Ekim M. Global left-ventricular function by tissue Doppler imaging in pediatric dialysis patients. Pediatr Nephrol 2008;23:779–785.
16. Rybczynski M, Koschyk DH, Aydin MA,Robinson PN, Brinken T, Franzen O, Berger J,Hofmann T, Meinertz T, von Kodolitsch Y,Tissue Doppler imaging identifies myocardial dysfunction in adults with Marfan syndrome. Clin Cardiol. 2007;30:19–24.
17. Rathe M, Carlsen NL, Oxhøj H. Late cardiac effects of anthracycline containing therapy for childhood acute lymphoblastic leukemia. Pediatr Blood Cancer. 2007;48:663-7.
18. Agricola E, Galderisi M, Oppizzi M, Schinkel AF, Maisano F, De Bonis M, Margonato A, Maseri A, Alfieri O. Pulsed tissue Doppler imaging detects early myocardial dysfunction in asymptomatic patients with severe mitral regurgitation. Heart 2004;90:406-10.